# FEM Analysis of Hybrid LTS/HTS Cos-theta Dipole Magnet with Heterogeneous Cable Model

A. D'Agliano, A. V. Zlobin, I. Novitski, D. Turrioni, E. Barzi, *Senior Member, IEEE,* S. Donati and V. Giusti

***Abstract*—The Lawrence Berkeley National Laboratory (LBNL) and the National High Magnetic Field Laboratory (NHMFL) have published results on Bi-2212 superconductive magnets realized and tested in the canted cosine-theta and solenoid designs, respectively. Fermilab is now preparing for the assembly of the first Bi-2212 stress-managed cosine-theta insert magnet. The insert will be part of the first hybrid cosine-theta magnet made of $Nb_3Sn$ outer layers within the US-MDP effort to reach a 20 T bore field. This paper presents the analytical analysis of the cosine-theta $Nb_3Sn$/Bi-2212 hybrid magnet. We report the parameters, logic, and implementation method of the 2D electromagnetic and mechanical FEM analysis of the LTS/HTS hybrid magnet. Results from a detailed heterogeneous model are compared to the homogeneous model implemented in the past. A Python code has been developed to simulate the current degradation due to stresses in the detail-modeled conductor areas. The current degradation has been introduced in the simulation dynamics for the HTS conductor as an iteration process, updating the input load of Lorentz forces of the energization at each step. The magnetic and mechanical analysis results of the 2D cosine-theta LTS/HTS dipole magnet have been described and analyzed.**

***Index Terms*—Accelerator dipoles, HTS coils, Finite element methods, Bi-2212 Wire, $Nb_3Sn$ Wire, Critical current.**

## I. Introduction

THE goal of the U.S. Magnet Development Program (MDP) [1] is to build the first hybrid cosine-theta dipole magnet and reach a bore field of 20 T [2]. Fermilab has designed a hybrid dipole made of two external layers of $Nb_3Sn$ and two internal layers of Bi-2212, with an aperture of approximately 15 mm [3].

The Bi-2212 compound is a promising HTS superconductor object of study to realize strands for high-field magnets for High Energy Physics applications [4]–[7]. The mechanical properties of Bi-2212 in a silver matrix, shaped in the Rutherford cable configuration, can be found in [8].

This paper presents the analytical study of two different Bi-2212 Rutherford cable-stack models: the homogenous and heterogeneous. We computed and compared the stress-strain curves between the two models at room temperature and at 4.2 K along the azimuthal and radial directions. We then used the validated heterogeneous model of the cable to perform the magnetic and mechanical analysis of the hybrid 4-layer dipole using ANSYS APDL. We implemented the stress and strain-induced current degradation in the Bi-2212 compound by connecting Python codes to the ANSYS APDL scripts. Simulation results are reported and discussed in the last section of this article.

This work is supported by Fermi Research Alliance, LLC, under contract No. under contract No. DE-AC02-07CH11359 with the U.S. Department of Energy and U.S. Magnet Development Program.

A. D'Agliano is with the Fermi National Accelerator Laboratory (FNAL), Batavia, IL 60510 USA and also with the University of Pisa, Pisa 56126, Italy (e-mail: dagliano@fnal.gov).

E. Barzi, I. Novitski, D. Turrioni and A. V. Zlobin are with the Fermi National Accelerator Laboratory, Batavia, IL 60510 USA.

S. Donati and V. Giusti are with the University of Pisa, Pisa 56126, Italy.

Manuscript received April 19, 2021; revised August 16, 2021.

## II. Bi-2212 Cable-Stack Analysis

### A. Homogeneous and Heterogeneous Cable Models

Experimental data are available for two different Bi-2212 stack samples: the strand and cable samples [8]. The strand sample was used to analyze the mechanical properties of a matrix of parallel Bi-2212 strands impregnated with epoxy CTD-101K. The cable sample was made of 5 Bi-2212 Rutherford cables piled in 2 identical stacks glued with epoxy, and was used to analyze the anisotropic behavior of the impregnated superconductor.

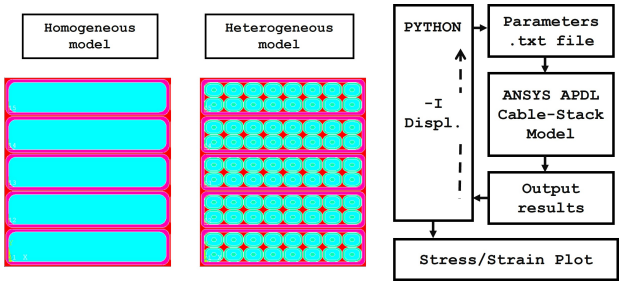


Fig. 1. Logical steps of the FEM analysis (right) implemented for both the homogeneous and the heterogeneous models (left).

This study compares two configurations of the Rutherford cable-stack model (Fig. 1, left). The first uses the homogeneous cable model characterized by mechanical properties experimentally determined from the strand sample [8]. The second uses the heterogeneous cable model where each structural material is assumed isotropic and bi-linear perfectly plastic [10]–[12]. We performed the ANSYS APDL mechanical analysis by applying symmetry boundary conditions on the right vertical surface of the cable-stack sample, coupled d.o.f. in y-direction for top surface nodes, and fully fixed constraints on the bottom surface. The simulation aimed to validate the Bi-2212 cable-stack heterogeneous model through comparison with the homogeneous cable model implemented with experimental material properties. Tables I and II show

the material properties from [8], [10]–[12] and used in the simulation for the homogeneous and heterogeneous models, respectively.

TABLE I
MECHANICAL PROPERTIES OF HOMOGENEOUS MODEL AT 300/4.2 K

| Properties value 300/4.2 K | Young Modulus [GPa] | Yield Stress [MPa] | Poisson ratio | Thermal Contraction [mm/m] |
|---|---|---|---|---|
| Hom. Cable | | | | |
| (radial) | 25.8/31.4 | 105 | 0.35 | 3.29 |
| (Azimuthal) | 25.8/31.4 | 105 | 0.35 | 2.9 |
| (Axial) | 50 | 105 | 0.35 | - |
| Epoxy | 13/20 | 790/1360 | 0.31 | 7.7 |

TABLE II
MECHANICAL PROPERTIES OF HETEROGENEOUS MODEL AT 300/4.2 K

| Properties value 300/4.2 K | Young Modulus [GPa] | Yield Stress [MPa] | Poisson ratio | Thermal Contraction [mm/m] |
|---|---|---|---|---|
| Bi-2212 | 21.26/21.26 | 120 | 0.4 | 3.29 |
| Silver | 83/91 | 54/80 | 0.395 | 4.32 |
| Epoxy | 13/20 | 790/1360 | 0.31 | 7.7 |

### *B. Compression Test at 300 K and 4 K.*

Fig. 2 shows the stress-strain curves for the Bi-2212 cable-stack sample, as computed in the homogeneous and heterogeneous models. We studied the compression along the azimuthal and radial directions at 300 K and after cool-down at 4.2 K. The logical steps of the FEM analysis are shown in Fig. 1 (right). Each sample was loaded with 13 increasingly larger displacements from 0 to 1.1%. After each iteration, the resulting reaction forces were stored in Python to generate the stress-strain curves.

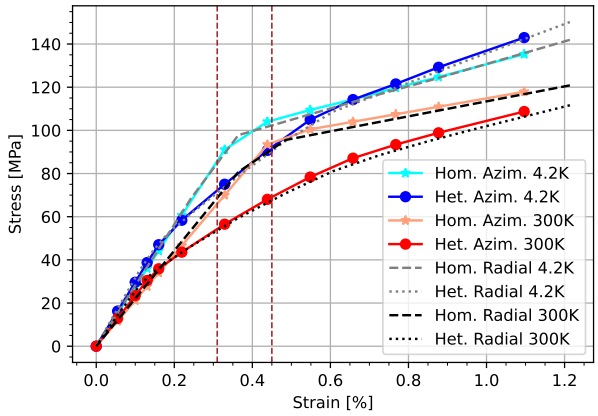


Fig. 2. Stress-strain curves for the Bi-2212 cable-stack samples, as computed in the homogeneous and heterogeneous models at the temperature of 4.2 K (in blue) and 300 K (in red). The vertical dashed red lines represent the lower and upper thresholds of current-degradation irreversibility [8].

The Bi-2212 Rutherford cable behaves as a very ductile material that constantly undergoes permanent plastic deformations, with a Young modulus that constantly decreases as the applied stress increases [8]. For this reason, the literature reports modeling studies that implement multi-linear plasticity or gasket material theories to model the Bi-2212 superconductor elements [9]. In this study, the heterogeneous model allowed us to obtain the described behavior, defining each structural material as isotropic and bi-linear perfect plastic (Fig. 2).

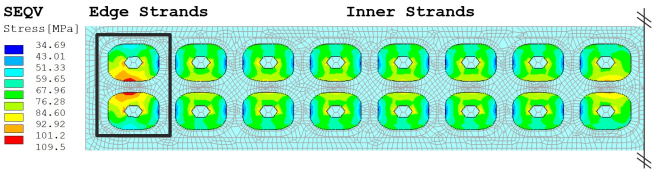


Fig. 3. Distribution of equivalent Von Mises stress in th e Bi-2212 Rutherford cable due to 100 MPa of transverse pressure at 4.2 K. The maximum stress of 109 MPa is found in the two edge strands (left). In the inner strands, the stress is lower due to the symmetry of the cable-stack sample.

Fig. 2 shows that the homogeneous and heterogeneous cable models behave identically for strain within zero and 0.2%. Moreover, their mechanical behavior remains similar for deformations close to the irreversibility threshold. This threshold is approximately 0.31% and is the percentage strain value for which the critical current degrades with permanent effects in the Bi-2212 strands. Without assuming any correlation between mechanical behavior and irreversibility strain, the homogeneous model shows a higher stiffness at room and cold temperatures above this threshold. The higher compliance of the heterogeneous model is due to portions of silver that reach plasticity at a stress intensity of 50 MPa at room temperature and 80 MPa at cryogenic temperature.

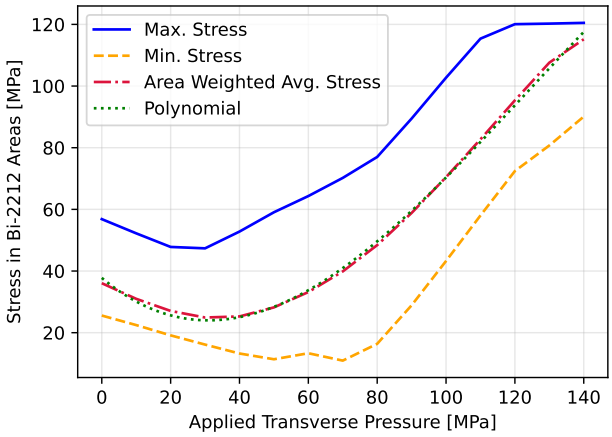


Fig. 4. Maximum, minimum, and area-weighted average stress computed in the Bi-2212 areas at the center of the cable-stack sample as a function of the applied transverse pressure. The interpolation of the weighted average stress curve provides an analytical form.

The heterogeneous model allowed for a precise estimate of the stress in the conductor areas as a function of the applied transverse pressure. Fig. 3 shows the stress distribution in the strands for a compression load of 100 MPa. To map the stress dependence on the applied transverse pressure (Fig. 4), we computed the maximum, minimum, average, and area-weighted average stress in the Bi-2212 areas of the specimen's central cable, the third one from the bottom. These quantities

show minima in the range from 20 to 70 MPa of applied transverse stress. This is due to the higher thermal contraction coefficient of the epoxy compared to Bi-2212 Rutherford cable, which undergoes radial compression during cool-down. When pressure is applied, the cable is compressed azimuthally, increasing the stress-state hydrostatic component in the strand nodes but reducing their Von Mises stress. We used the area-weighted average stress to estimate the effect of current degradation due to the transverse pressure in the mechanical simulation of the 4-layer hybrid dipole.

## III. Hybrid 4-layer SMCT Dipole Magnet

### A. Magnetic and Mechanical Analysis

We performed the magnetic and mechanical simulation of the 4-layer hybrid cosine-theta dipole magnet. Fig. 5 (left) reports a simple scheme of the simulation's logical steps. We developed a Python interface to write the input file for the ANSYS APDL codes, read the output files, and analyze the results.

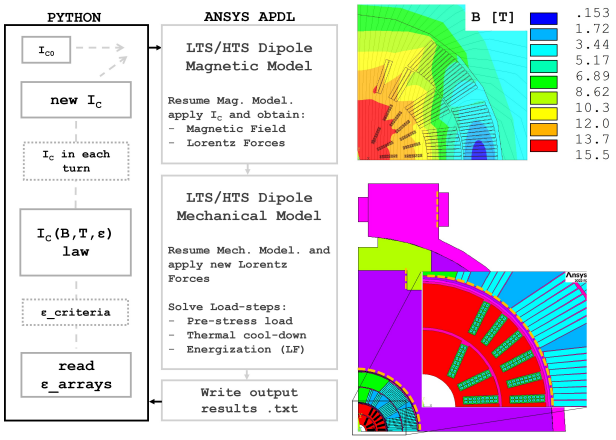


Fig. 5. The logical steps of the simulation (left). Dipole magnetic model (right, top) and mechanical structure of the 4-layer hybrid cosine-theta dipole magnet: two inner layers of Bi-2212 and two outer layers of $Nb_3Sn$ (right, bottom).

We performed the simulation using the ANSYS element `PLANE 53` for the magnetic analysis and `PLANE 183` for the mechanical analysis. Table III reports the mechanical properties of the construction materials used in the simulation and collected from the literature [10]–[12]. Standard contacts were allocated at the interfaces between the HTS mandrel and Bi-2212 impregnation material and between pole/wedges and $Nb_3Sn$ epoxy insulation. Pre-stress interference loads were chosen in the range of 50-100 $\mu m$ and were inserted between the outer layer of the HTS coil and the skin, the outer layer of the LTS coil and the iron yoke, the aluminum clamp and the iron yoke, and the stainless steel shell and the bolt.

### B. Stress/Strain-induced Current Degradation

To compute the strain-induced current degradation in the dipole coil, we used the following analytic law [13], [14]:

$$\Delta I_C/I_{C0}(\varepsilon) = \begin{cases} \alpha\varepsilon, & \text{if } \varepsilon < \varepsilon_{irr} \\ \beta\varepsilon + \varepsilon_{irr}(\alpha - \beta), & \text{if } \varepsilon > \varepsilon_{irr} \end{cases} \quad (1)$$

TABLE III
Mechanical Properties of Dipole Materials

| | Properties value 300/4.2 K | | |
|---|---|---|---|
| | **Young Modulus [GPa]** | **Poisson ratio** | **Thermal Contraction [mm/m]** |
| Bi-2212 | 21.26/21.26 | 0.4 | 3.29 |
| Silver | 83/91 | 0.4 | 4.32 |
| $Nb_3Sn$ rad. | 35/40 | 0.3 | 2.87 |
| $Nb_3Sn$ azim. | 20/40 | 0.3 | 3.3 |
| Inconel-718 | 208/219 | 0.29 | 2.43 |
| Brass | 105/120 | 0.31 | 3.17 |
| Titanium | 108/125 | 0.31 | 1.66 |
| G10 | 19/23 | 0.31 | 2.46 |
| SS304 | 199/210 | 0.27 | 3.05 |
| Kapton | 2.5/2.5 | 0.34 | 20.7 |
| Iron | 205/225 | 0.29 | 2.07 |
| Aluminum | 70/81 | 0.31 | 4.0 |

where $\varepsilon$ is the percentage strain, and the parameters values are $\alpha = -2.7$, $\beta = 100 \cdot \alpha$ and $\varepsilon_{irr} \approx 0.32\%$. In this case, irreversibility was not implemented. The strain $\varepsilon$ is determined from the mechanical analysis output: a value of element-averaged strain is obtained for each Bi-2212 cable area. The criterion adopted to interpret the complex strain state in the cables significantly affects the study. For this reason, both the Von Mises equivalent strain and the total mechanical and thermal strain intensity were chosen and compared according to the following definitions [15]:

$$\varepsilon_{\text{eqv}} = \frac{\sqrt{\frac{1}{2}[(\varepsilon_1 - \varepsilon_2)^2 + (\varepsilon_2 - \varepsilon_3)^2 + (\varepsilon_3 - \varepsilon_1)^2]}}{(1+\nu)} \quad (2)$$

$$\varepsilon_{\text{int}} = \min(|\ \varepsilon_1 - \varepsilon_2\ |, |\ \varepsilon_2 - \varepsilon_3\ |, |\ \varepsilon_3 - \varepsilon_1\ |) \quad (3)$$

where $\varepsilon_1$, $\varepsilon_2$ and $\varepsilon_3$ are the tensor principal strains, independent from the reference system, and $\nu$ is the material Poisson's ratio. Concerning the output stress, the same criteria were used as for the output strain.

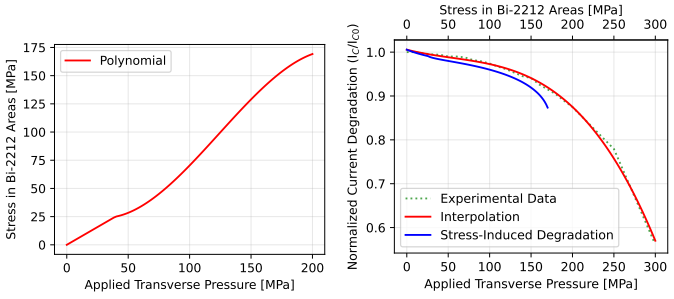


Fig. 6. Polynomial interpolation of the area-weighted average stress in the Bi-2212 area from eq. (4) (left). Normalized current degradation as a function of applied transverse pressure in red from [16], and as a function of stress in the Bi-2212 areas in blue (right).

To evaluate the stress-induced current degradation in the HTS coil, we obtain a function that directly associates the area-weighted average stress in Bi-2212 areas with the normalized current degradation. To do so, the expression of the polynomial interpolation from the plot in Fig. 4, was numerically inverted,

and then the function of current degradation due to transverse pressure was applied, interpolating the experimental data. In the range 40-170 MPa, the cubic polynomial interpolation that returns the area-weighted average stress in the Bi-2212 areas as a function of the applied transverse pressure is:

$$y = ax^3 + bx^2 + cx + d \tag{4}$$

where $y$ is the area-average stress, $x$ is the transverse pressure, with coefficients: $a = -4.642 \times 10^{-5}$, $b = 1.724 \times 10^{-2}$, $c = -0.9338$ and $d = 37.77$. Below 40 MPa of transverse pressure, the linear dependence $y = 0.63 \cdot x$ was assumed to avoid computational issues without compromising the quality of the analysis. The function of current degradation due to transverse pressure was obtained by interpolating the experimental data from [16], considering Sample 4 (LBNL2002). The coefficients of the cubic polynomial expression are: $a = -2.378 \times 10^{-8}$, $b = 3.899 \times 10^{-6}$, $c = -4.816 \times 10^{-4}$ and $d = 1.006$. Fig. 6 shows the plots related to the polynomial functions described above. The blue line represents the combined function that returns the current degradation as a function of the stress in the Bi-2212 area. Eventually, that function was applied in the Python code to evaluate the current drop in each coil turn while the area-weighted average stress in the HTS coil (Fig. 7) changes during iterations.

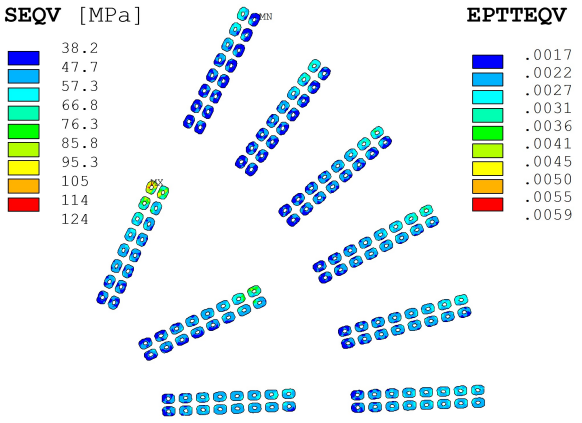


Fig. 7. Max equivalent Von Mises stress (left, MPa), and total mechanical and thermal strain intensity (right) on the Bi-2212 areas at the first iteration step of the mechanical analysis (at 4.2 K and 8 kA).

Fig. 8 reports the stress and strain-induced current degradation results in the hybrid cosine-theta dipole magnet. The interpretation of the current drop at the beginning of each iteration is that the current of powering is set to $I_{C0}$. The current drop at step $k$ is evaluated as a percentage of $I_{C0}$ and not as a percentage of the $I_C$ value evaluated at step $k-1$. Hence, the $I_C$ convergence result strongly depends on the $I_{C0}$ value set as the initial critical current.

## IV. Conclusion

Implementing the heterogeneous Rutherford cable model improves the quality of the magnetic and mechanical ANSYS simulations. This paper validates the heterogeneous model by comparing the stress-strain curves along the radial and azimuthal directions to the corresponding curves obtained in

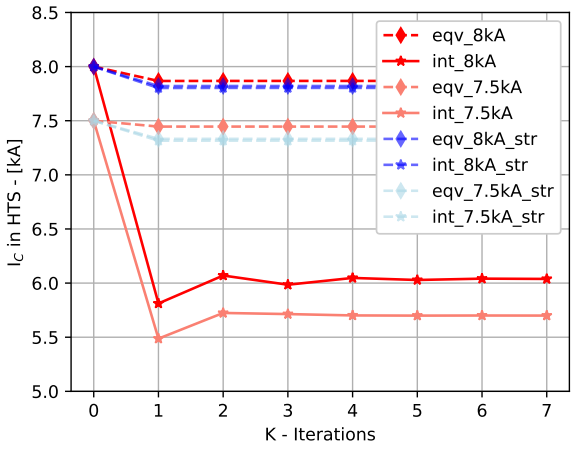


Fig. 8. Strain (red) and stress (blue) induced current degradation in the Bi-2212 Rutherford coil. Curves were computed by applying different stress-strain criteria and different initial critical currents.

the homogeneous model. The two simulations show almost identical mechanical behavior for a strain percentage between zero and 0.2%. For higher values of the strain percentage, the homogeneous model is characterized by a stiffer behavior. The validated heterogeneous model and its material properties were used for the magnetic and mechanical analysis of the hybrid 4-layer cosine-theta dipole magnet developed at Fermilab. The mechanical results of stress and strain in the Bi-2212 areas allowed us to estimate the stress and strain-current degradation [13], [14], [16]. Applying the law of strain-induced current degradation with total mechanical and thermal strain intensity criteria, the current drop was 24.5% at $I_{C0}$ = 8 kA, with an average of 23.6% between 8 and 6 kA. The strain intensity criterion is the most conservative ($\varepsilon_{\text{int}}$). If the Von Mises criterion is applied, the current drops only by 1.7% at 8 kA and 0.7% at 7 kA. Using the stress-induced current degradation law, for $I_{C0}$ = 8 kA, we obtained a current drop of 2.5% with the stress intensity criterion and 2.2% with the Von Mises criterion.

In conclusion, we can state that stress and strain-induced current degradation have mild effects unless the most conservative criterion is considered. The same analysis was performed for the hybrid dipole modeled with the homogeneous Rutherford cable. The results further underestimate the current degradation effect, highlighting the importance of the heterogeneous model, which allows the obtaining of a more detailed stress/strain state at the strand level. The model implemented can be extended to other types of superconductors, and the results can be a valuable tool for magnet designers to optimize the magnet cross-section and minimize the current degradation in future particle physics accelerators.

## Acknowledgments

This work was supported by the EU Horizon 2020 Research and Innovation Program under the Marie Sklodowska-Curie Grant Agreement No. 734303, 822185, 858199 and 101003460, and the Horizon Europe Research and Innovation Program under the Marie Sklodowska-Curie Grant Agreement No. 101081478.

## REFERENCES


[1] U.S. Magnet Development Program Website. "https://usmdp.lbl.gov/".

[2] P. Ferracin, and others. "Conceptual Design of 20 T Hybrid Accelerator Dipole Magnets". IEEE Transitions on Applied Superconductivity, Vol. 33, No. 5, 2023.

[3] A. V. Zlobin, I. Novitski, E. Barzi. "Conceptual Design of a HTS Dipole Insert Based on Bi2212 Rutherford Cable". Instruments, Vol. 4, 2020.

[4] T. Shen, A.V. Zlobin, D. Larbalestier. "White Paper on High Temperature Superconducting Bi-2212 Magnets for Energy Frontier Circular Colliders". Accelerator Physics, contribution to Snowmass 2021. https://doi.org/10.48550/arXiv.2203.10564

[5] A. V. Zlobin, I. Novitski, E. Barzi, Senior Member, IEEE, and D. Turrioni. "Development of a Bi2212 Dipole Insert at Fermilab". IEEE Transactions on Applied Superconductivity, Vol. 33, No. 5, August 2023

[6] L. Garcia Fajardo et al. "First demonstration of high current canted-cosinetheta coils with Bi-2212 Rutherford cables". Supercond. Sci. Technol., Vol. 34, 2021.

[7] Shen, T., Bosque, E., Davis, D. et al. Stable, predictable and training-free operation of superconducting Bi-2212 Rutherford cable racetrack coils at the wire current density of 1000 A/mm2. Sci Rep 9, 10170 (2019).

[8] P. Li, Y. Wang, A. Godeke, L. Ye, G. Flanagan and T. Shen, "Thermal-Mechanical Properties of Epoxy-Impregnated Bi-2212/Ag Composite," in IEEE Transactions on Applied Superconductivity, vol. 25, no. 3, pp. 1-4, June 2015, Art no. 8400904, doi: 10.1109/TASC.2014.2376178.

[9] Eric Qiuli Sun. "Multi-scale nonlinear stress analysis of $Nb_3Sn$ superconducting accelerator magnets". Superconductor Science and Technology, 2022, Vol. 35.

[10] David R. Smith and F. R. Fickett, *Low-Temperature Properties of Silver*, Vol. 100, Number 2, March–April 1995, Journal of Research of the National Institute of Standards and Technology.

[11] E. Barzi, *Conductor Properties and Coil Technology for a Bi2212 Dipole Insert for 20 Tesla Hybrid Accelerator Magnets*, Contribution to Snowmass 2021, Oct. 2022, [Online]. Available: https://doi.org/10.48550/arXiv.2204.01072

[12] NIST Cryogenics Material Properties Database. "https://trc.nist.gov/cryogenics/materials/materialproperties.htm"

[13] N. Cheggour, X. Lu, T. Holesinger, T. Stauffer, J. Jiang, L. Goodrich (2011). "Reversible effect of strain on transport critical current in Bi 2Sr 2CaCu 2O 8+x superconducting wires: A modified descriptive strain model". Superconductor Science and Technology. 25. 015001. 10.1088/0953-2048/25/1/015001.

[14] M. Sugano, K. Itoh, T. Kiyoshi. "Strain Dependence of Critical Current in Bi2212 W & R Wires Under Magnetic Field Up to 30 T". IEEE Transactions on Applied Superconductivity, Vol. 16, 2006.

[15] ANSYS Mechanical User's Guide. "https://ansyshelp.ansys.com/public/account/secured?returnurl=/Views/Secured/corp/v242/en/wb_sim/ds_Home.html"

[16] A. Kario, S. Otten, S. Wessel, J. Bijlsma, M. Smithers, H. ten Kate, A. Ballarino (University of Twente), T. Shen (LBNL), U. Trociewitz, D. Davis, E. Bosque, D. Larbalestier (FSU/NHMFL). "Transverse stress susceptibility of Bi-2212 Rutherford cables at 4.2 K and 11 T". US-MDP Collaboration Meeting, Fermilab, 2024.